Freestanding Arrays of Nanowire Materials for High Rate Capability Battery Electrodes

W. C. West, N. V. Myung, J. F. Whitacre, and B. V. Ratnakumar

Electrochemical Technologies Group/Micro Device Laboratory

Jet Propulsion Laboratory
California Institute of Technology
Pasadena, CA

December 2002

Motivation: Micro Power Sources for Space Exploration

- Need for highly miniaturized power sources:
  - Many proposed NASA missions call for use of a number of small, compact vehicles for exploring a great variety of environments
    - Cold, hot, high g, high radiation, sun-obscured...
    - Long life characteristics highly desirable (includes shelf life)
  - Will enable/prolong planetary exploration, to permit novel science missions
- JPL development includes many aspects of micro power:
  - Power storage: Miniaturized batteries and electrochemical capacitors
  - Power generation: Micro thermoelectrics, a-voltaics
  - Power conversion: Micro inductors for DC-DC conversion
- Technology Insertion Opportunities
  - Miniaturized penetrators e.g. Deep Space II
  - Aerobots
  - Small rovers
  - Autonomous/distributed sensors

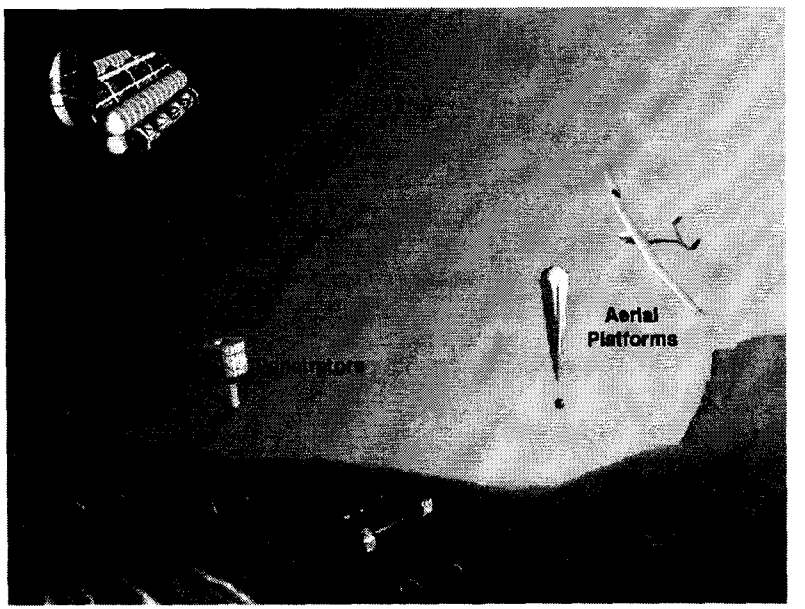

Motivation

- Batteries/electrochemical capacitors with high power density electrodes are useful for many space applications (e.g. data transmission bursts, pyro initiation)
- Nanowire electrodes are possible candidate materials for high power density applications:
  - Very high rate capability demonstrated for some materials[1]
  - No binder
  - Little conductive additive (just substrate contact)
- Prior Art:
  - Sol-gel based V_2O_5, SnO_2, $LiMn_2O_4$, $LiFePO_4$[2]
  - Manufacturing/scale-up to practical electrodes is non-trivial
- Synthesize state of the art lithium primary/secondary cathode materials and electrocapacitor electrodes via process amendable to scale-up

[1]N. Li, C. R. Martin, and B. Scrosati, *Electrochem. and Solid State Lett.,* **3** 316 (2000).
[2]for example: F. Croce, C. Sides, B. Scrosati, and C. R. Martin, abstract 172, *May 2002 Meeting of the Electrochemical Society.*

Materials System Under Consideration

Battery Materials:

Primary:

•MnO_2 specific capacity: 310 mAhr/g

Secondary:

•a-MnO_2*xH_2O specific capacity: 440 mAhr/g[1]

•$LiCoO_2$ specific capacity: 140 mAhr/g,

•$LiNi_{0.8}Co_{0.2}O_2$ specific capacity: 180 mAhr/g

Electrochemical Capacitor Materials:

IrO_2

MnO_2, MnO_x

NiO, Co_3O_4

[1]J. J. Xu, A. J. Kinser, B. B. Owens, and W. H. Smyrl, *Electrochem. Solid State Lett.*, **1**, 1(1998).

Alumina Nanotemplating Approach for Nanowire Array Fabrication

Advantages:

- Uniform anisotropic morphology, self-organized at the nanometer scale
- Ability to control pore size (few nm to 200 nm)
- Can be integrated with other silicon fabrication processes, scaleable
- Ability to fabricate thick templates (up to 200 microns)
- High pore density (10^9-10^{12})
- Highly ordered pore arrangement
- High temperature tolerance (up to 600°C), high chemical and mechanical stability

Anodizing Controlling Parameters:

- Applied Potentials or Current Density
- Anodizing Solution Compositions:
  - Sulfuric Acid, Oxalic Acid, Chromic Acid, Phosphoric Acid
- Temperature
- Agitation

Cross Sectional View of Alumina Nanotemplate on a Silicon Wafer

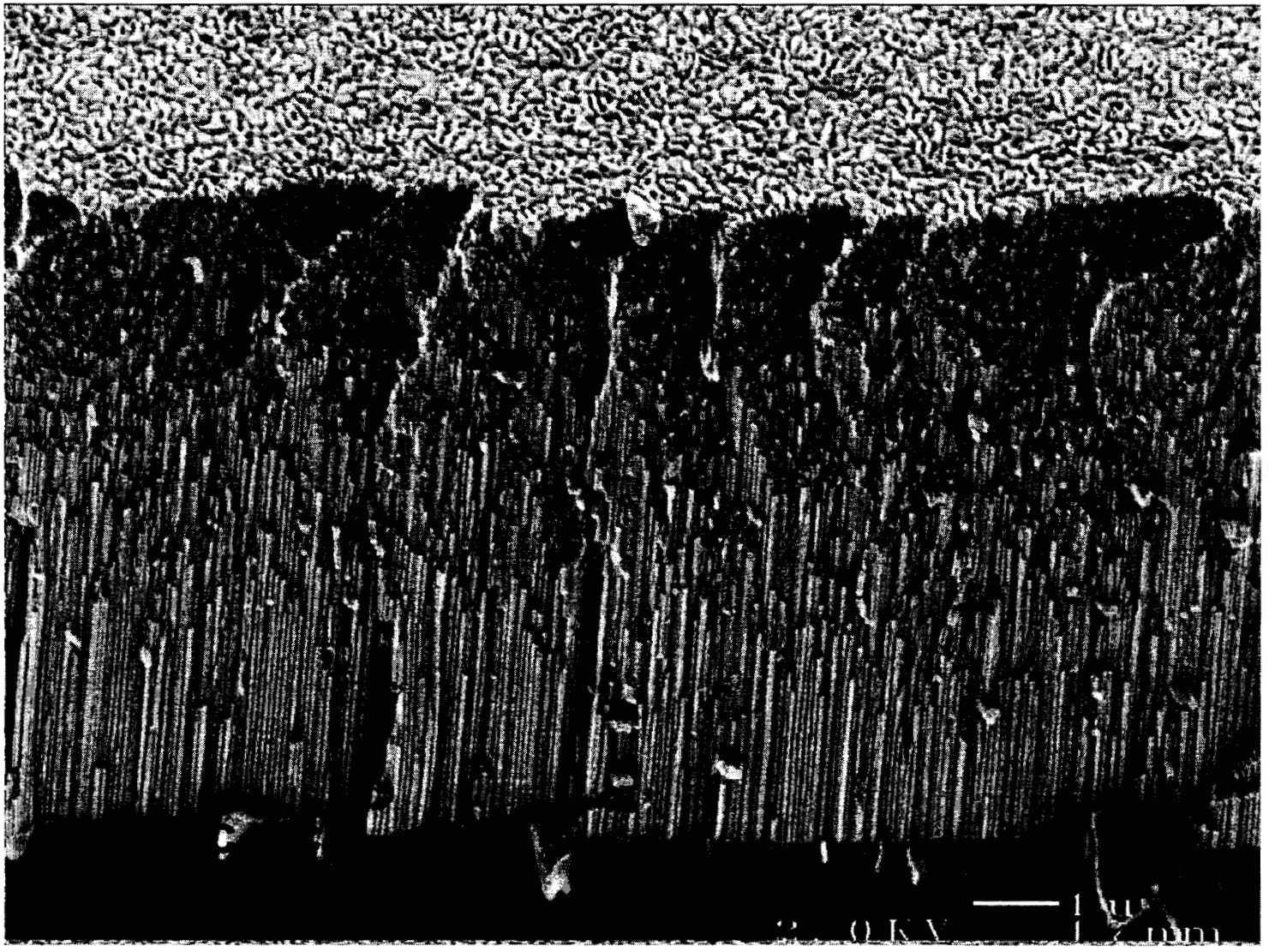

Alumina Nanotemplate Fabrication Steps on Silicon Wafers

E-beam evaporated 5 to 25 μm Al + 5 nm Ti on highly doped silicon wafer

1st Anodizing (Disordered)

Removal of 1st anodized alumina
8% CrO_3 + 20 % H_3PO_4 (1:1)

2nd Anodizing (Ordered)

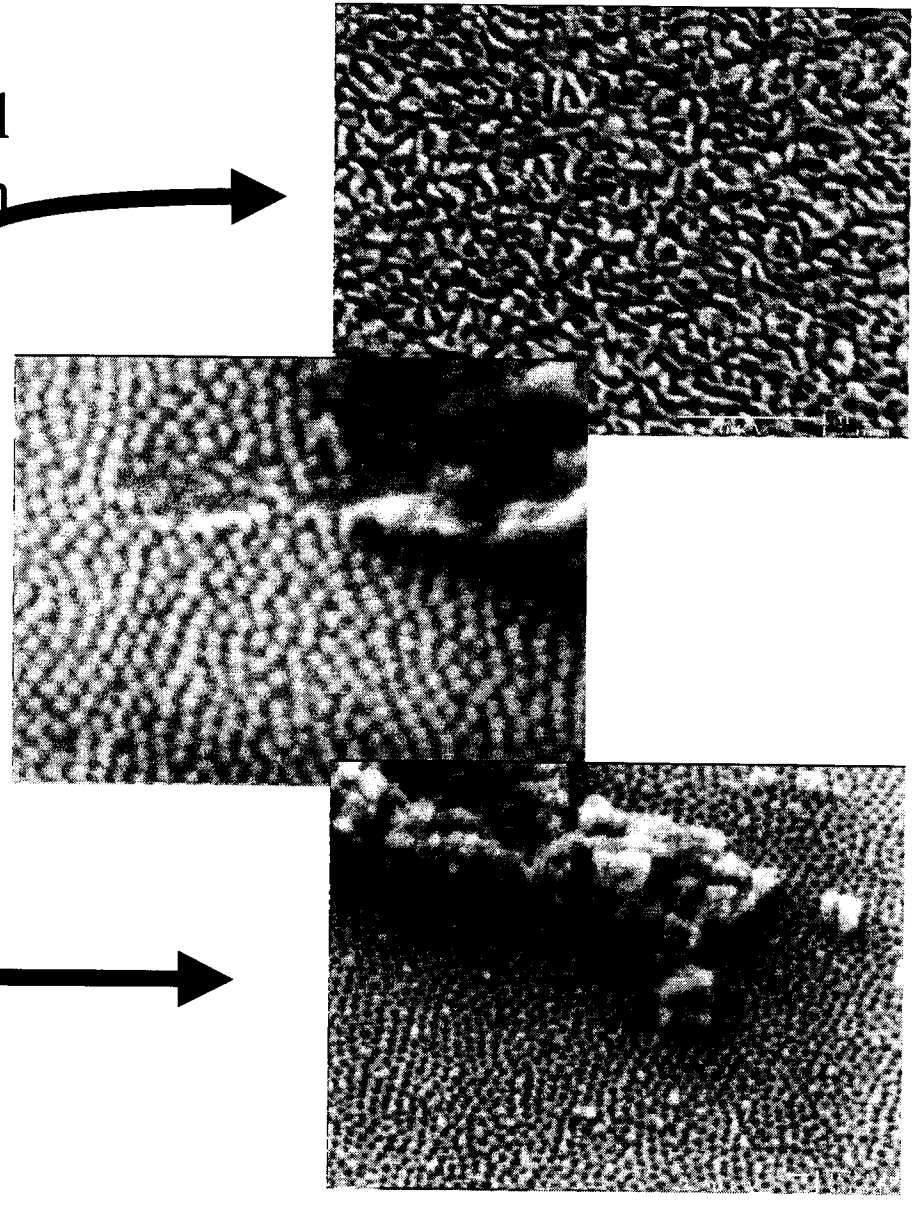

Pore Size vs. Applied Potentials in Sulfuric Acid

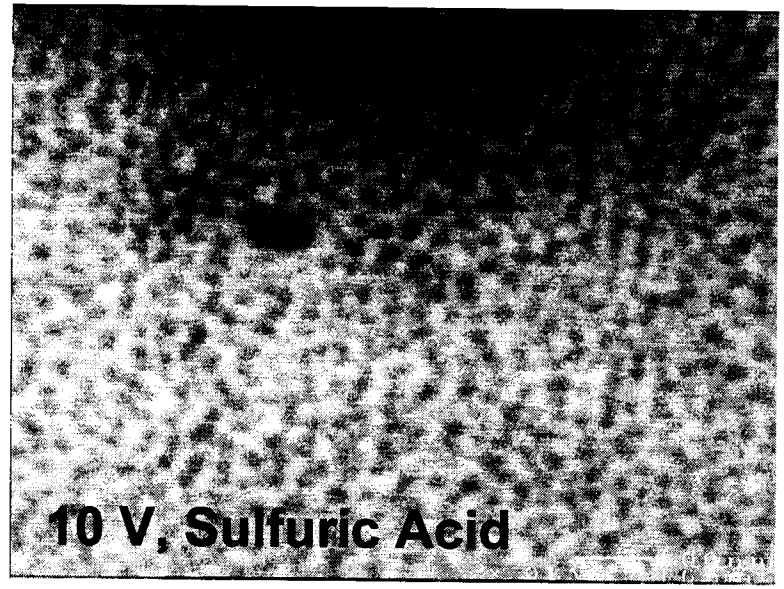

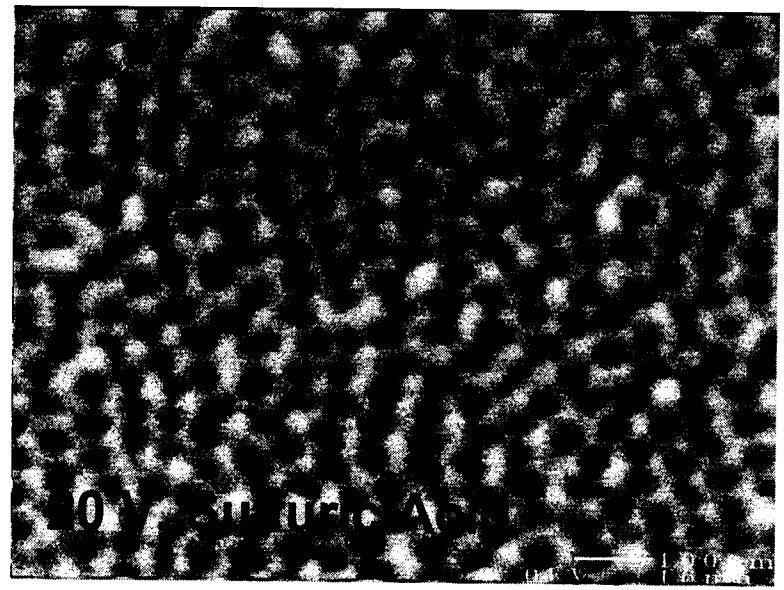

Pore Size vs. Applied Potentials in Oxalic Acid

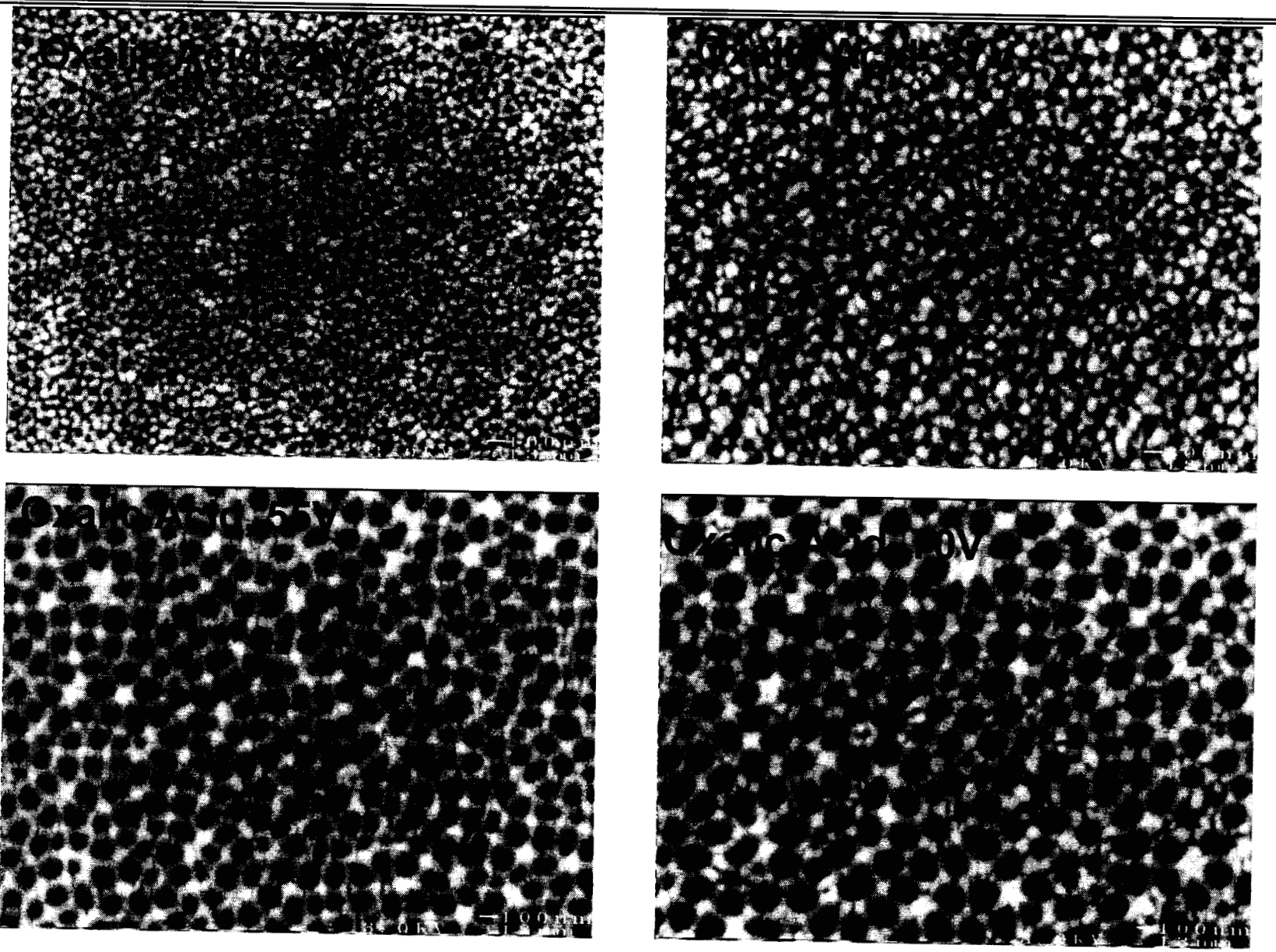

Pore Size and Porosity of Alumina Nanotemplates vs. Applied Potentials

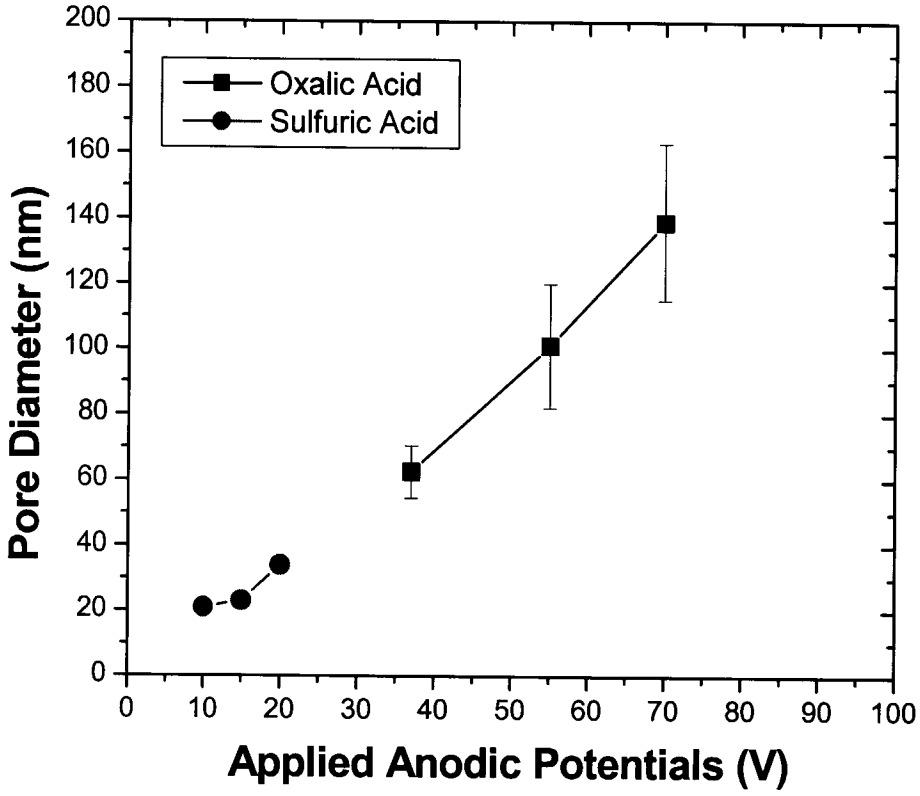

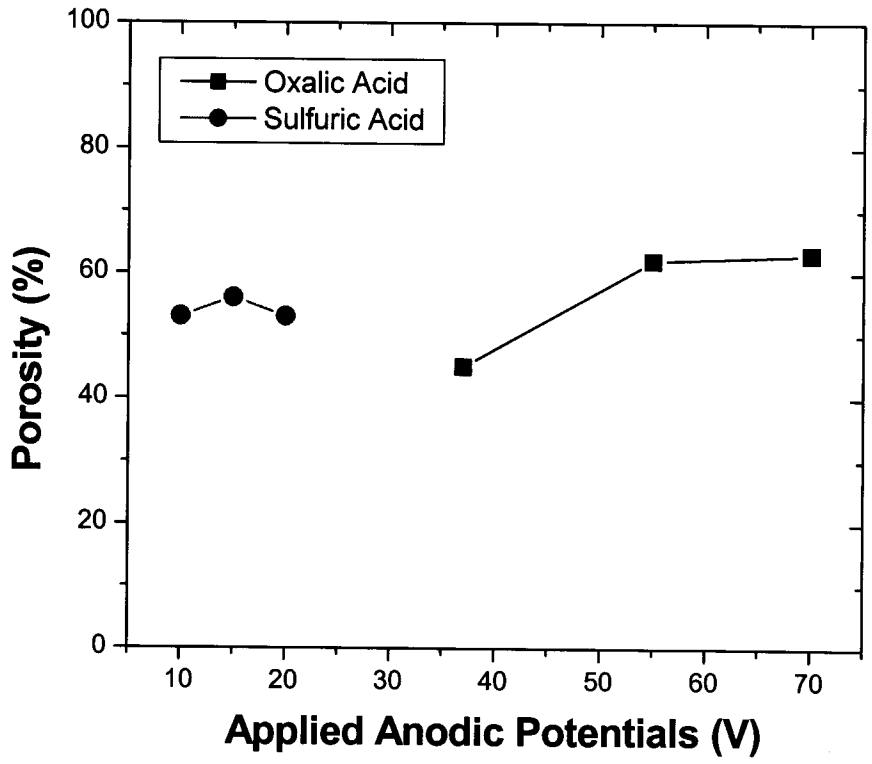

Fabrication processes for Nanoengineered Materials

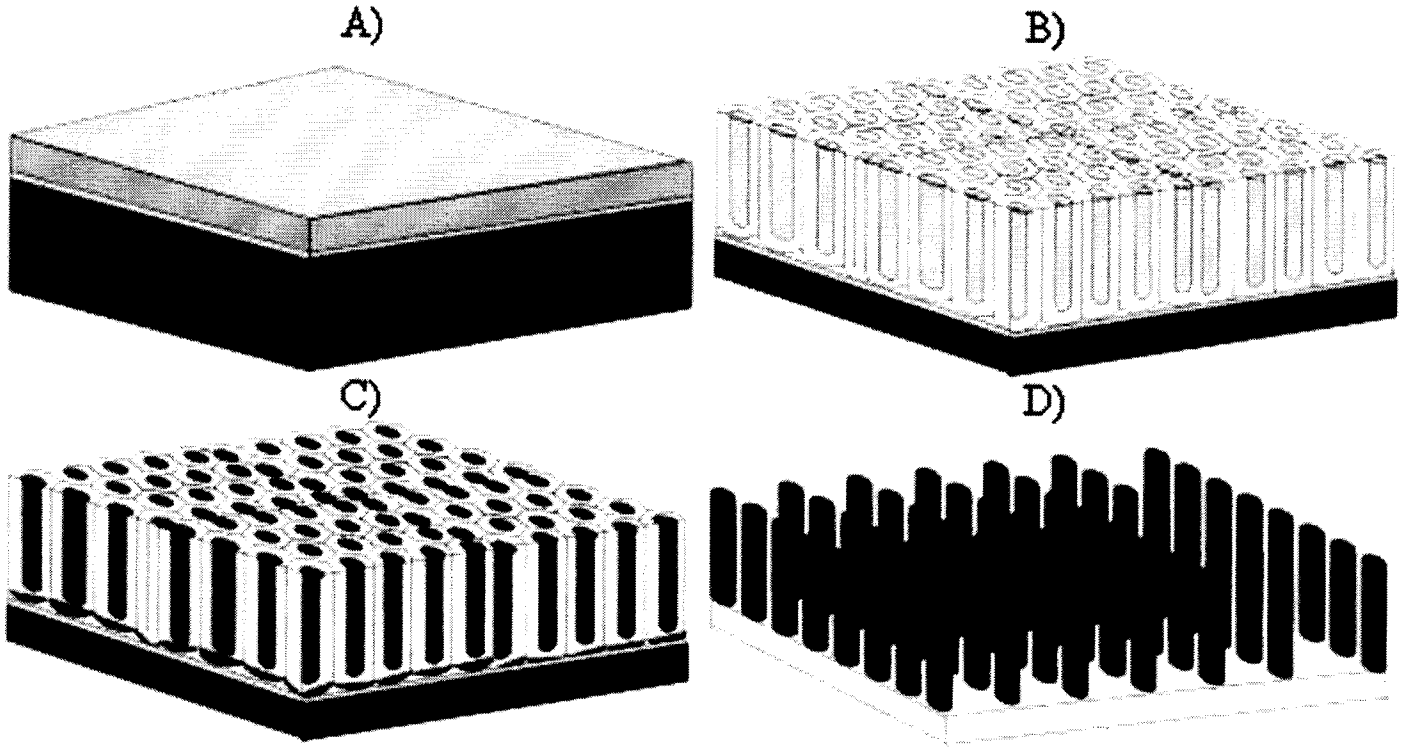

Fabrication process for nanoengineered materials using alumina nanotemplates: A) Al e-beam evaporated Si substrate with Ti adhesion layer, B) anodized Al, C) electrodeposited active material, D) removal of alumina nanotemplate

Nanowire Synthesis: Electrodeposition of metallic nanowires

- Co-Ni oxide nanowires:
- Sputter deposit Au contact to commercially supplied nanoporous alumina template (nominal pore size = 100 nm)
- Mount on C tape
- Electrodeposit $Co_xNi_{(1-x)}$ wires:
  - $CoSO_4 + NiSO_4 + Na_2SO_4 + H_3BO_3$ + Saccharin at 10 mA/cm^2
  - pH = 3, adjusted with HCl, H_2SO_4, NaOH or NH_4OH

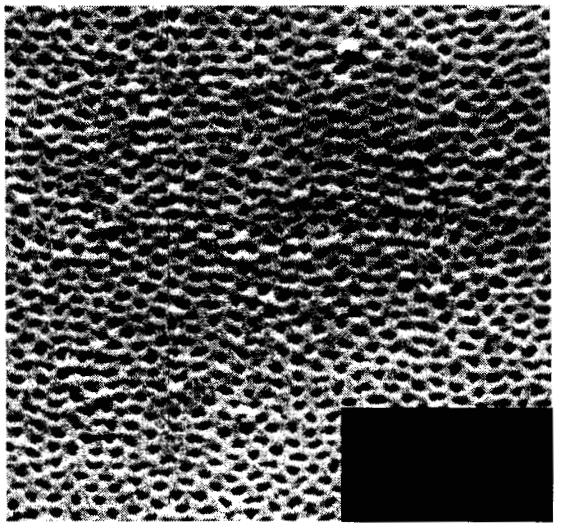

JPL fabricated nanoporous alumina template

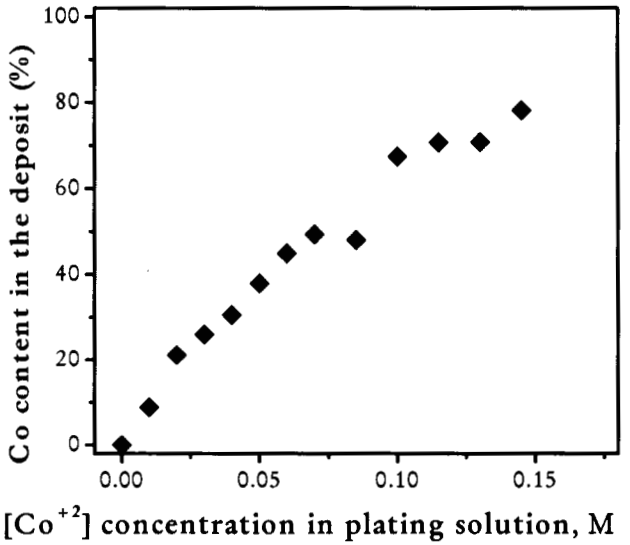

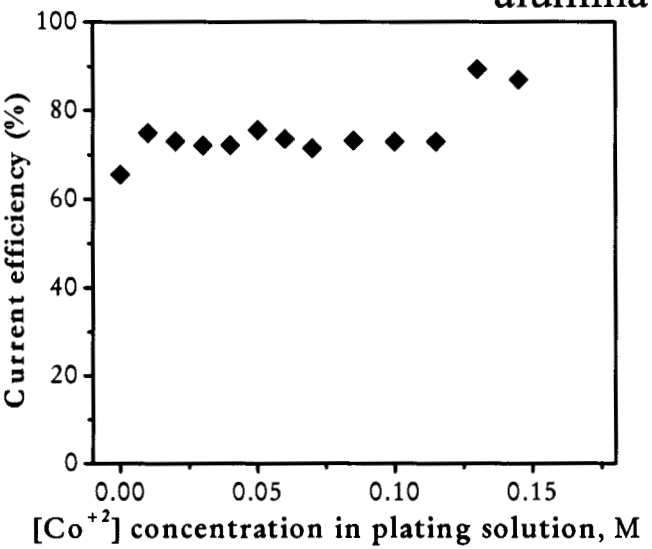

Nanoporous Alumina Template Effects

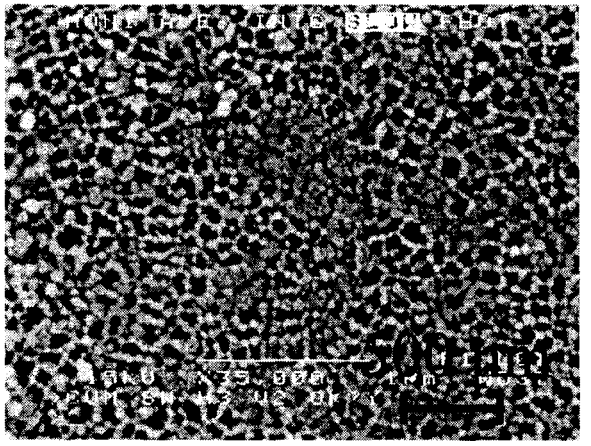

Whatman Anodisc (100 nm pores)

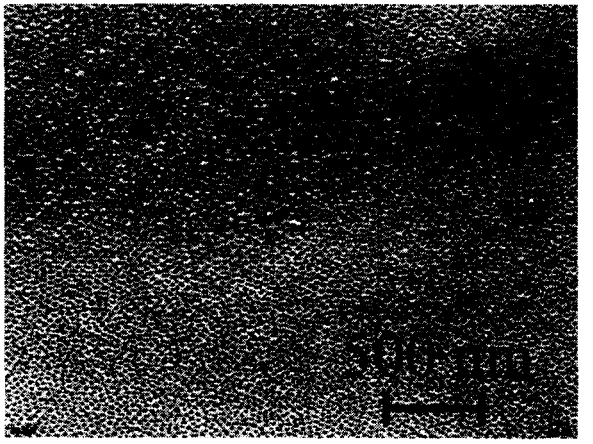

JPL synthesized alumina template (20 nm pores)

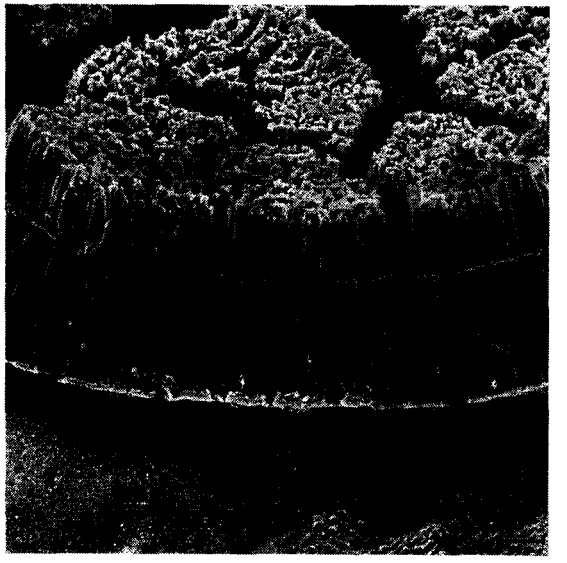

- Rate capability of nanowire electrodes will be a function of nanowire diameter and spacing.
- Partially undigested alumina template results in incomplete conversion to metal oxide nanowires.

Nanowire Synthesis: Anodic oxidation/crystallization

- Digest template in 1M NaOH, leaving freestanding Co, Ni nanowires on Au film
- Soak in deionized H_2O to remove NaOH between nanowires
- anodically oxidize Co or Ni in 4 M LiOH at 1 mA/cm^2
- Anneal in air at 300-800°C to crystallize metal oxide nanowires
- Mount onto Pt coated SiO_2 substrate with Ag paste

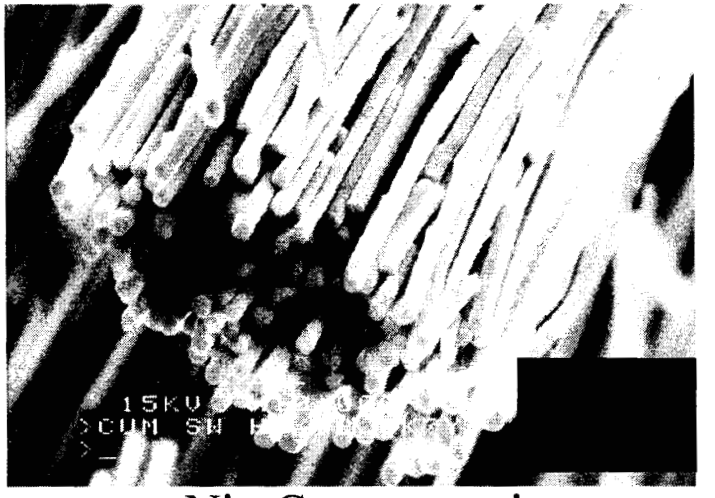

$Ni_{0.8}Co_{0.2}$ nanowires

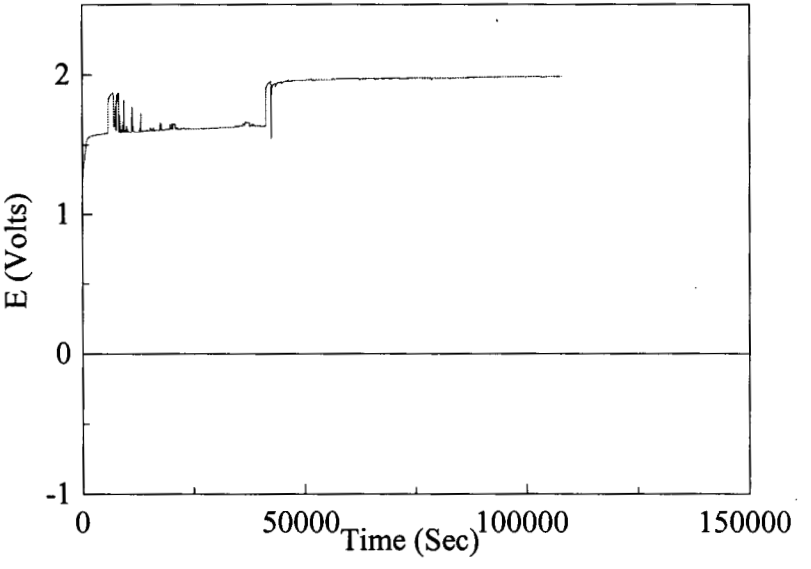

Anodic oxidation of Co nanowires

Nanowire Synthesis: Electrodeposition of Metallic Nanowires

Energy Dispersive Spectrometry Study:
Co/Ni ratio = 12.4%/87.6%

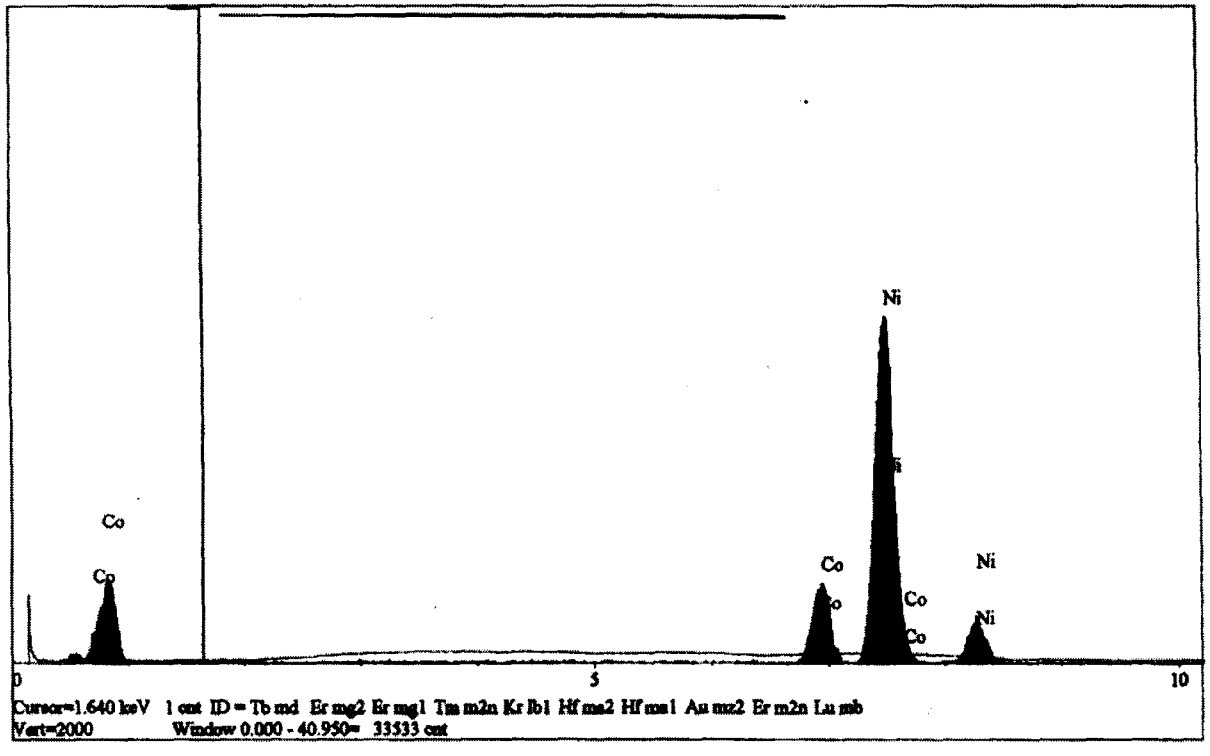

<u>Results:</u> Co/Ni ratio = 12.4%/87.6%

Nanowire Synthesis: Oxidation of Metallic Nanowires

X-ray Diffraction Study: Co_3O_4

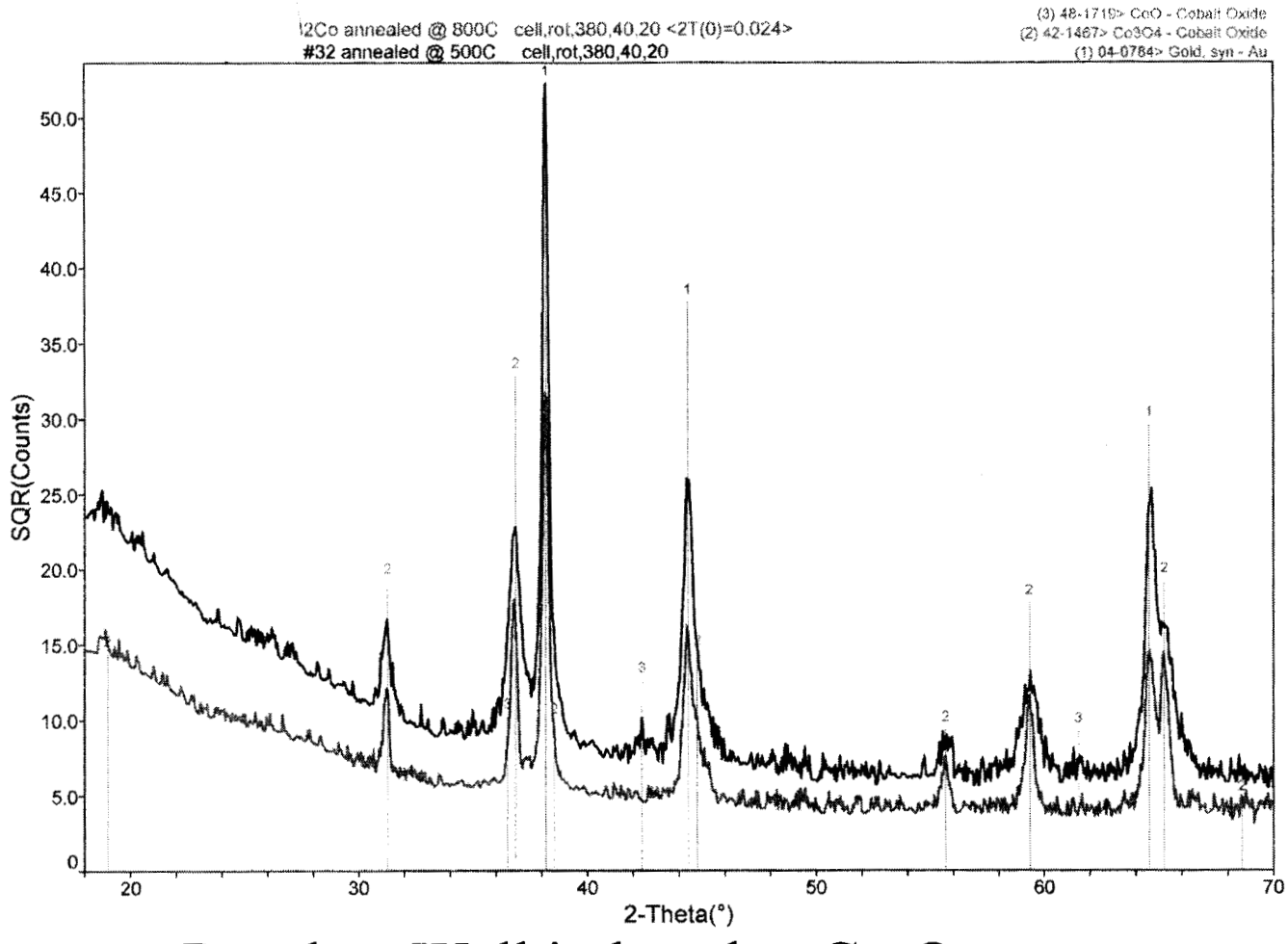

<u>Results:</u> Well indexed to Co_3O_4

Nanowire Synthesis: Oxidation of Metallic Nanowires

X-ray Diffraction Study: NiO

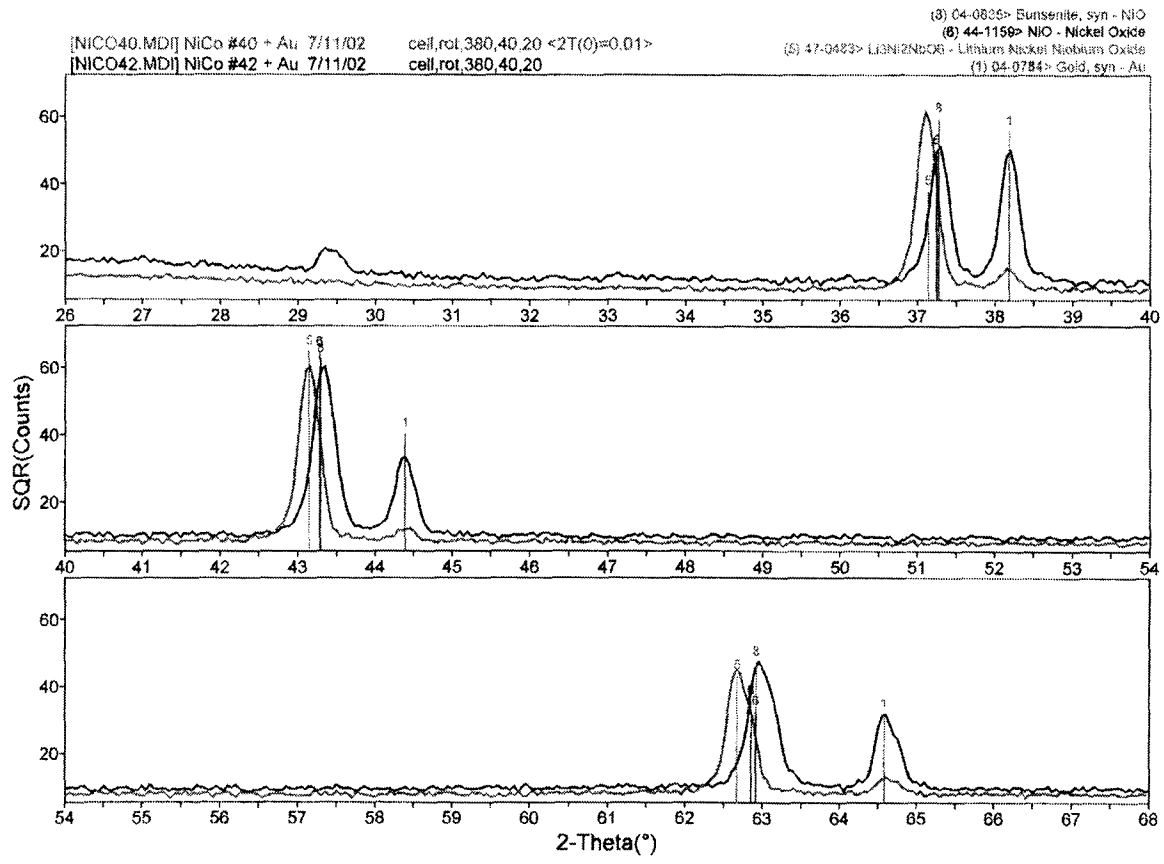

<u>Results:</u> Well indexed to NiO

Nanowire Synthesis: Oxidation of Metallic Nanowires

X-ray Diffraction Study: Co oxide, annealed and unannealed

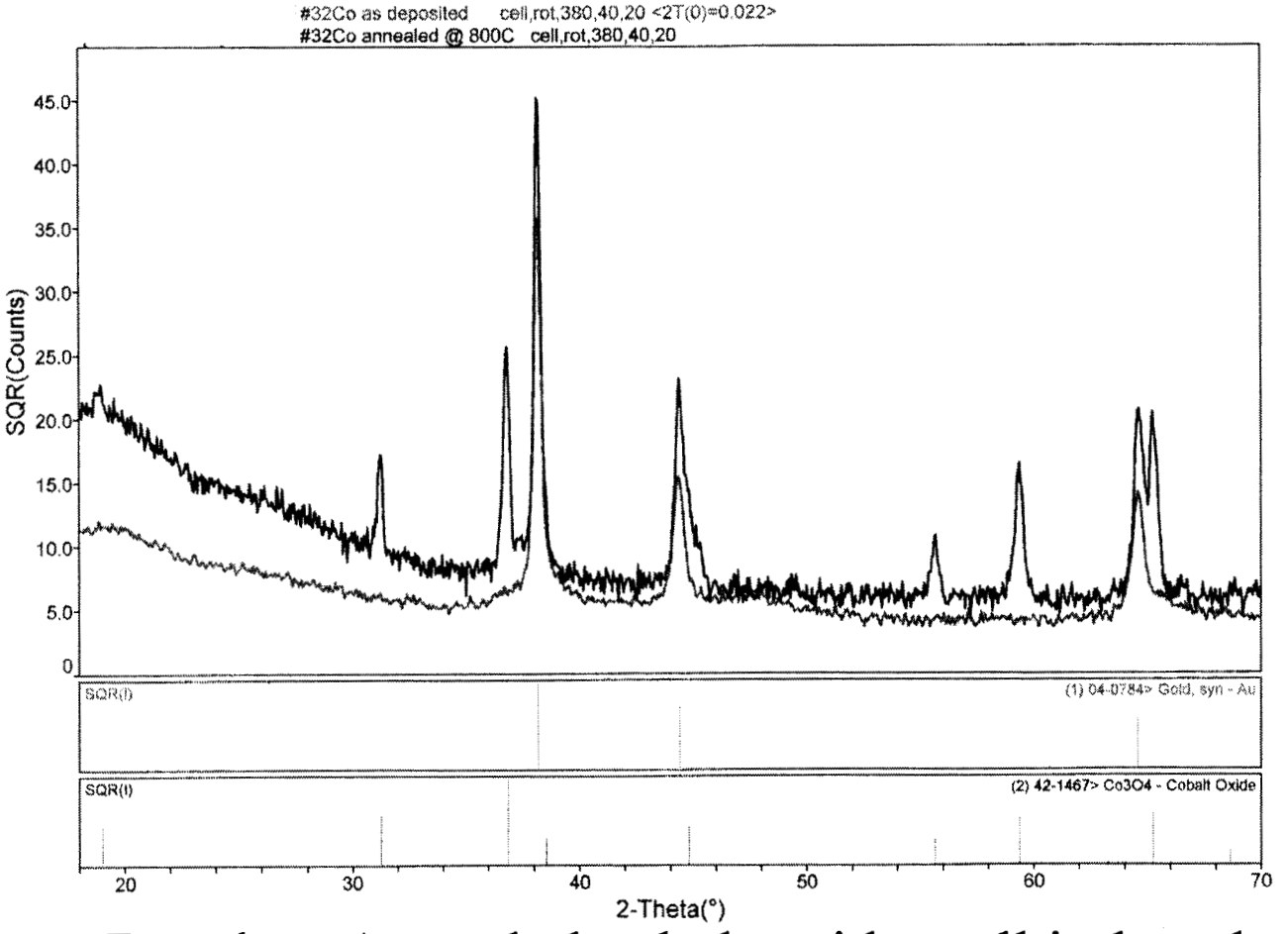

<u>Results:</u> Annealed cobalt oxide well indexed to Co_3O_4, unannealed is amorphous

Direct MnO_x Potentiostatic Electrolysis

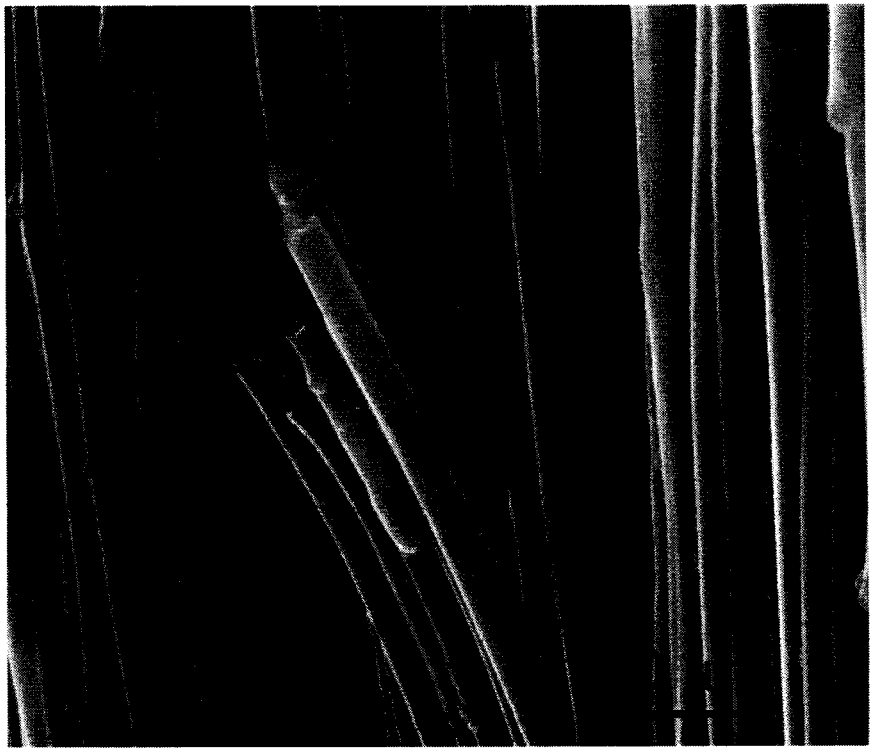

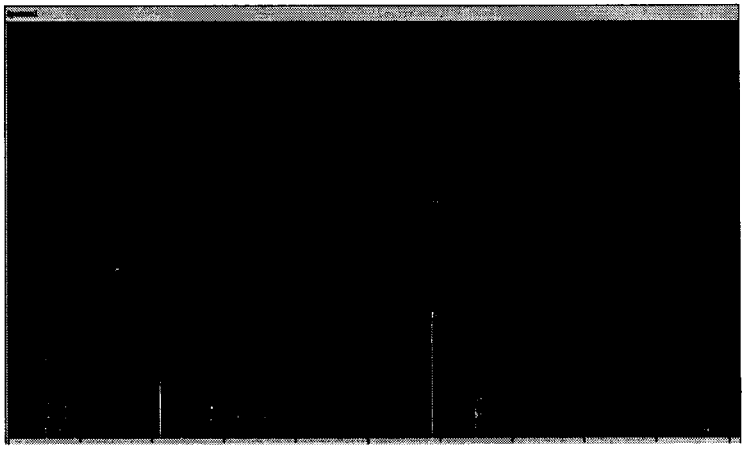

MnO_x electrolysis:

- Sputter deposit in Au coated alumina templates
- Deposition bath: $MnSO_4 + (NH_4)_2SO_4$
- pH = 8 by addition of H_2SO_4 or NH_4OH
- E_{dep} = 0.2-1.2V vs. SCE

Direct MnO_x Potentiostatic Electrolysis

XPS Characterization of MnO_x: O 1S

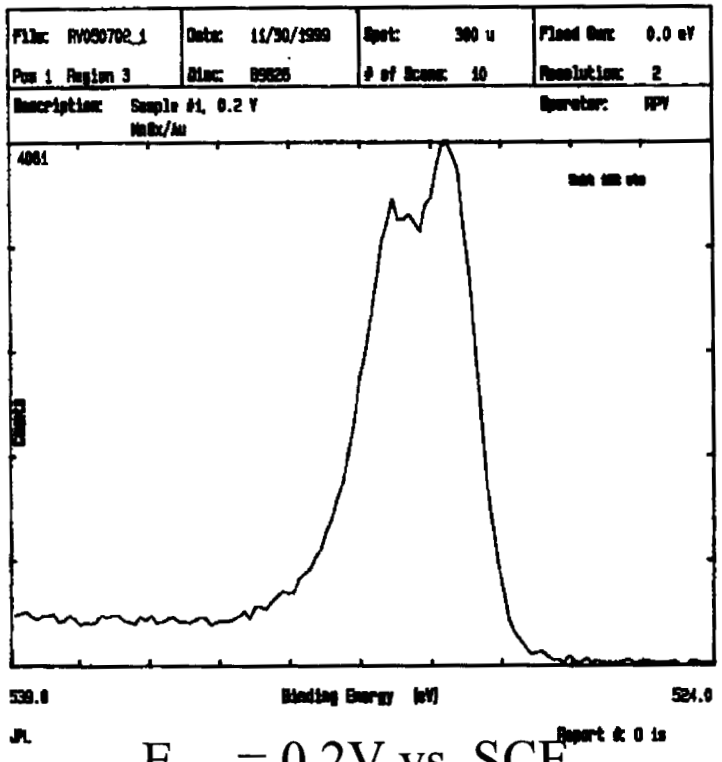

E_{dep} = 0.2V vs. SCE
Mixed valence Mn

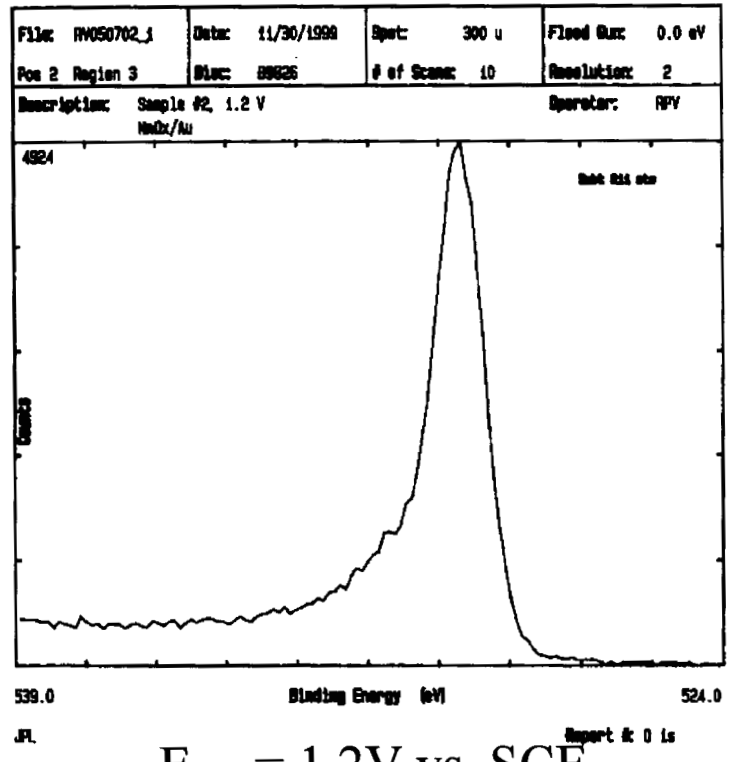

E_{dep} = 1.2V vs. SCE
Single valence Mn

Composition of manganese oxide nanowires can be tailored via potentiostatic control[4]

[4]M. Chigane and M. Ishikawa, *J. Electrochem. Soc.*, **147**, 2246 (2000).

Battery Cycling Data: MnO_2*xH_2O vs. Li

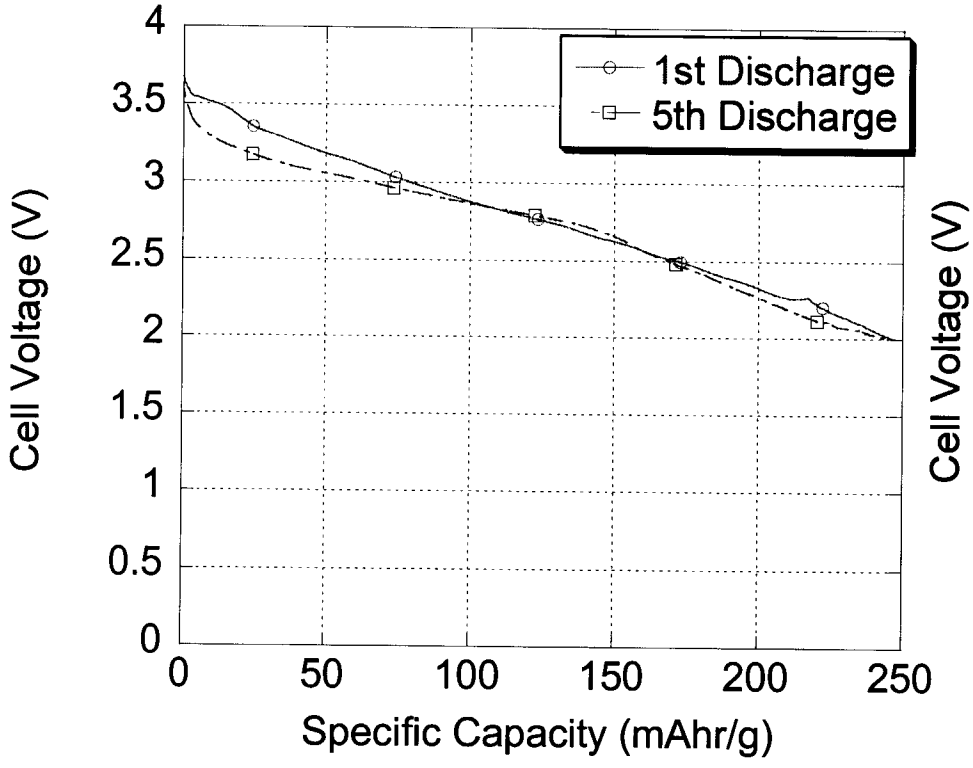

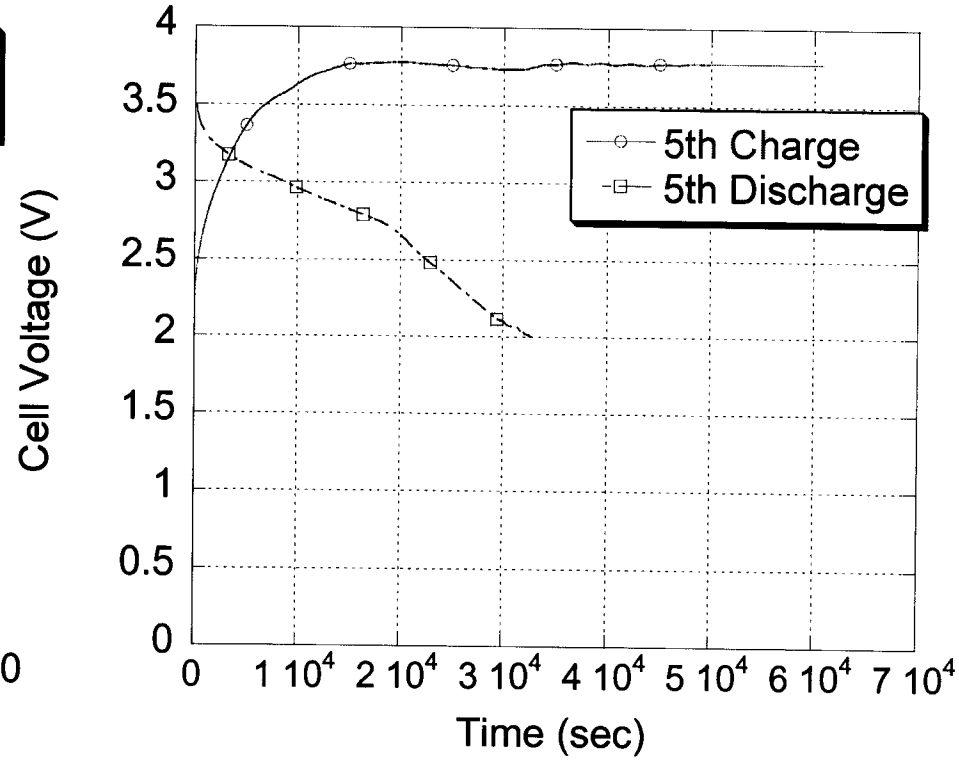

Cathode: area = 1.3 cm^2, no binder, no conductive additive
Nanowires: length = 6.5 μm, diameter = 0.1 μm, porosity = 43%
Anode: Li foil
Electrolyte: 1M $LiPF_6$ in PC
Discharge Rate: 50 μA

Capacitor Data: Co Oxide Nanowires

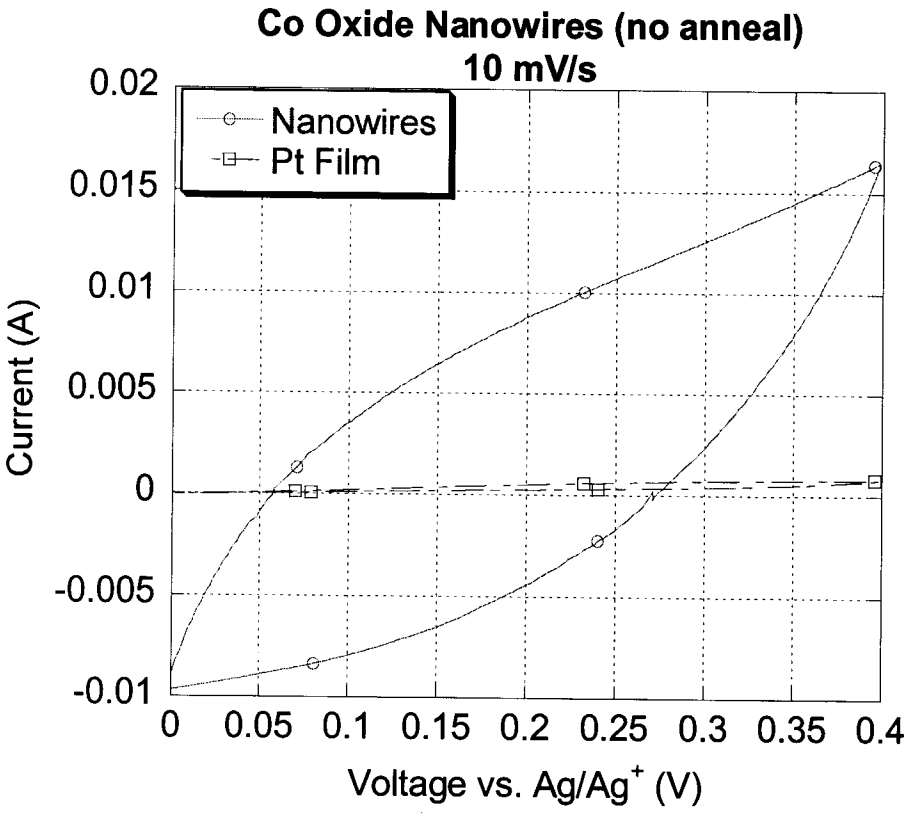

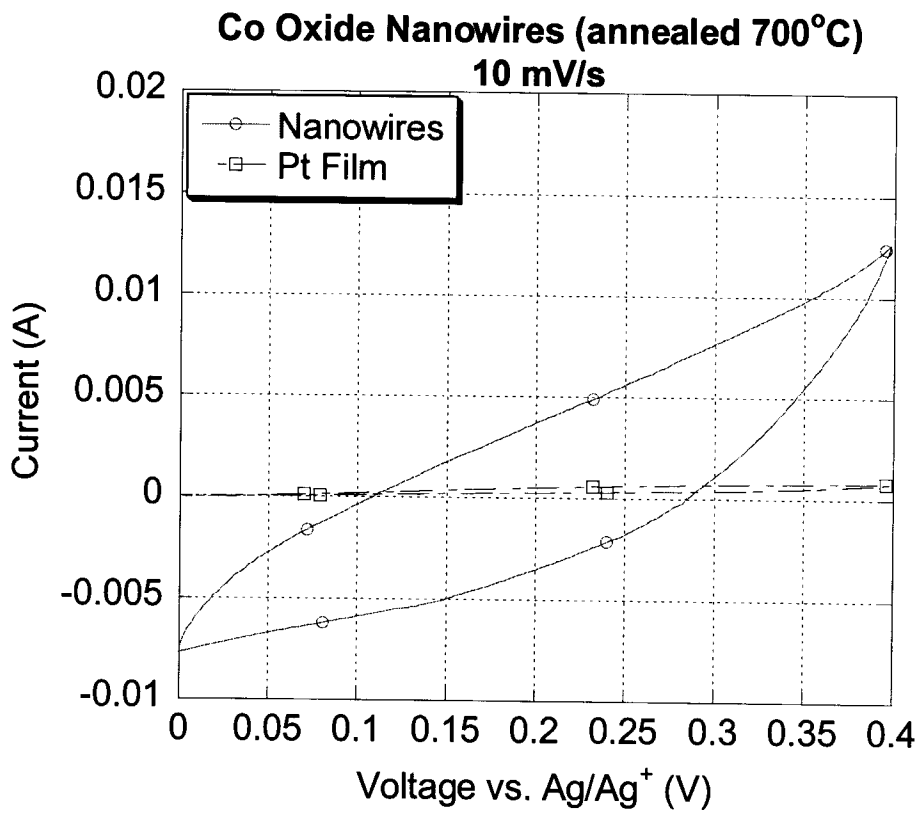

Nanowire electrode: area = 1.3 cm^2, no binder, no conductive additive
Nanowires: length = 10 μm, diameter = 0.1 μm, porosity = 43%
Counter electrode: Pt film on SiO_2
Electrolyte: 1M KOH in DI H_2O

Capacitor Data: Ni Oxide Nanowires

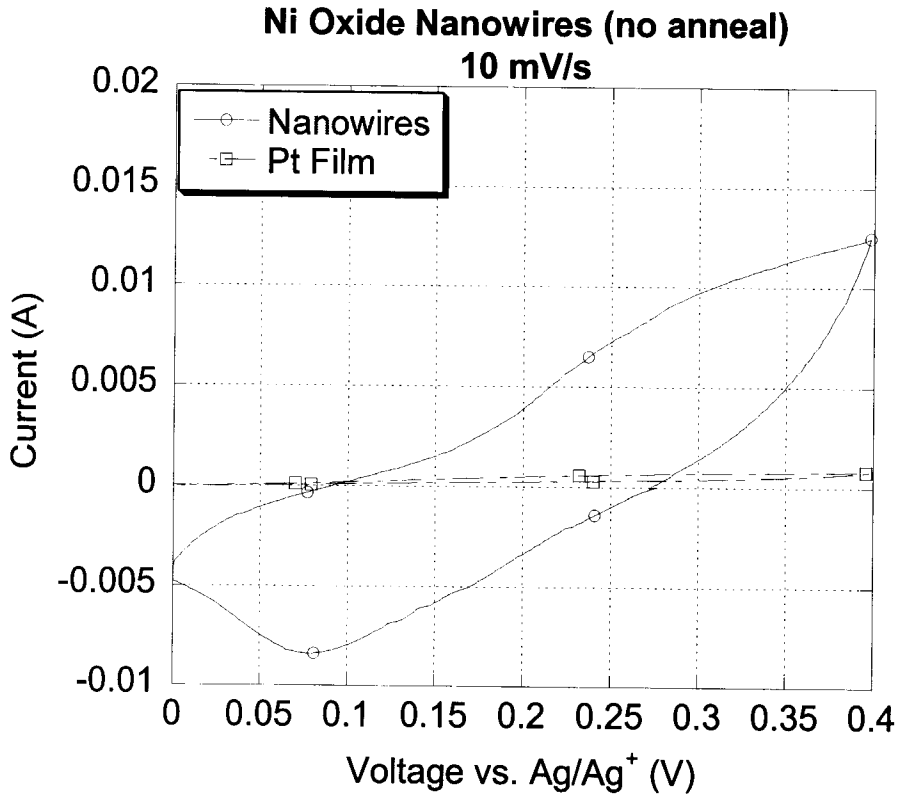

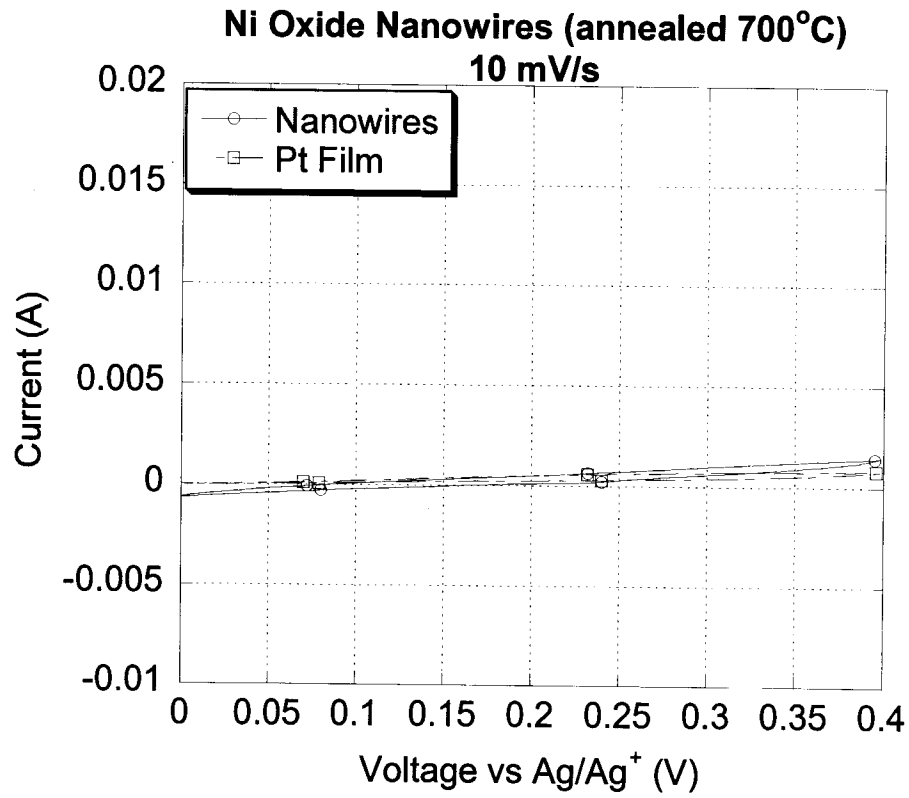

Nanowire electrode: area = 1.3 cm^2, no binder, no conductive additive
Nanowires: length = 10 μm, diameter = 0.1 μm, porosity = 43%
Counter electrode: Pt film on SiO_2
Electrolyte: 1M KOH in DI H_2O

Capacitor Data: Ni Oxide Nanowires

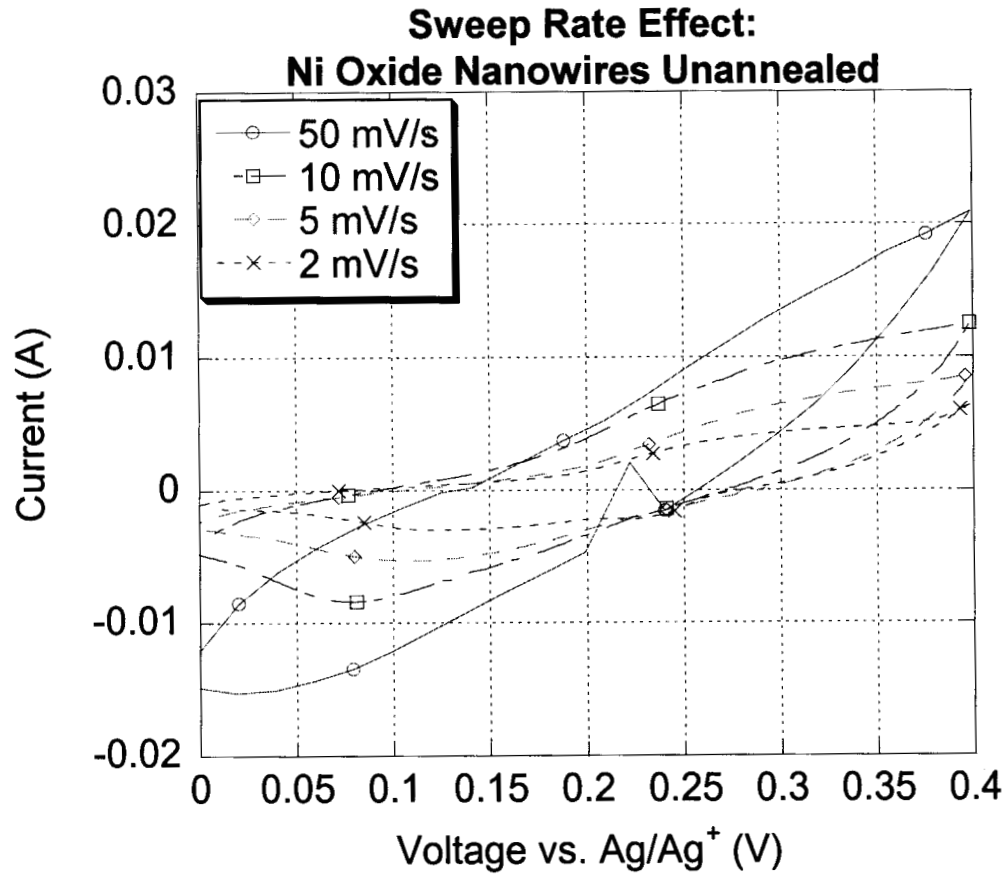

Nanowire electrode: area = 1.3 cm^2, no binder, no conductive additive
Nanowires: length = 10 μm, diameter = 0.1 μm, porosity = 43%
Counter electrode: Pt film on SiO_2
Electrolyte: 1M KOH in DI H_2O

Summary

- New nanowire synthesis methods have been used to prepare arrays of freestanding nanowires of electrochemically active materials:
  - Anodic oxidation of metallic nanowires in aqueous Li^+ solutions and subsequent annealing
  - Potentiostatic electrolysis of manganese oxides
- Functional batteries using nanowire electrodes demonstrated:
  - ➢ $Li:MnO_2*xH_2O$ battery system has attractive specific capacity, capable of multiple charge/discharge cycles
- Functional electrochemical capacitors demonstrated:
  - ➢ Co_3O_4 and NiO nanowire electrodes are viable electrochemical capacitor materials
- Future work will focus on further improving rate capability of nanowire electrodes for the $LiCoO_2$ and MnO_2*xH_2O / Co_3O_4 NiO/IrO_2 nanowires

Acknowledgements

This work was carried out at the Jet Propulsion Laboratory of California Institute of Technology under contract with the National Aeronautics and Space Administration. The authors acknowledge the financial support of the JPL Director's Research and Development Fund and the NASA Cross Enterprise Research and Development Fund.

The authors thank Ron Ruiz for providing SEM and EDS measurements, Jim Kulleck for providing the XRD measurements, and Rick Vasquez for providing the XPS measurements.